Computer Science Depatrment of The University of Auckland
CITR at Tamaki Campus (http://www.tcs.auckland.ac.nz)

CITR-TR-33 November 1998

Height from Gradients in Polar Coordinates

Jin Luo [1] and Karsten Schlüns [2]

Abstract

This paper presents a new approach to integrate the gradient field to the relative depth or height map from multiple view directions in polar coordinates. Traditional integration techniques are based on cartesian coordinates. In this approach, the surface normals are calculated by photometric stereo method. The object is illuminated by three light sources and rotated on a controlled turntable. The experimantal results of the cross section of the synthetic and real objects are feasible and promising.

[1] The University of Auckland, Computer Science Department, CITR, Tamaki Campus (Building 731), Glen Innes, Auckland, New Zealand
[2] University Hospital Charite, Humboldt University, Berlin, Germany

Height from Gradients in Polar Coordinates

Jin Luo [1] **and Karsten Schlüns** [2]

[1] CITR, University of Auckland
Tamaki Campus, Building 731, Auckland, New Zealand

[2] University Hospital Charité, Humboldt University, Berlin, Germany

Abstract: This paper presents a new approach to integrate the gradient field to the relative depth or height map from multiple view directions in polar coordinates. Traditional integration techniques are based on cartesian coordinates. In this approach, the surface normals are calculated by photometric stereo method. The object is illuminated by three light sources and rotated on a controlled turntable. The experimental results of the cross section of the synthetic and real objects are feasible and promising.

Keywords: gradient field, polar coordinates, integration techniques, photometric stereo

1 Introduction

Surface reconstruction in computer vision attempts to recover the physical parameters of the visual world, such as the depth or orientation of a surface. The 3D vision task consists of a sequences of steps, first transforming 2D digital images to surface characteristic descriptions (orientations) and into a 2.5D reconstructed depth map, then merging a set of depth maps to a full 3D representation. The recovered surface shape can be applied in different context, for instance location, recognition, surface inspection in industry as well as 3D visualisation and animation in computer graphics.

There are several shape from shading methods, such as 3S (three light sources) photometric stereo, resulting in surface gradient fields [1, 3]. This surface information still has to be transformed into relative height or depth maps, or into surface data for many industrial and commercial applications. However, integration techniques for gradient field have not been very well studied so far. Essentially there are two types of known discrete integration techniques - local propagation methods and global optimisation methods in cartesian coordinates [2, 3].

Local integration-path methods [5, 7, 10, 9] are directed on a local calculation of height increments by curve integrals. They differ in specifying an integration path and a local neighbourhood. Whereas, integration of gradient fields is thought to be an optimisation problem in global techniques [8, 6]. Global optimisation integration can also be regarded as a variational problem where a certain functional has to be minimised.

Generally, local path methods are easy to implement and do not explicitly implement any assumption of the integrability condition. However, the locality of computations strongly depends on data accuracy, and the propagation of errors may occur due to the propagation of height increments along paths. Comparing with the local path integration, the global optimisation methods are more robust against noise and produce better qualitative reconstruction for real objects, especially for curved objects. Nevertheless, the integration condition has to be assumed for the global techniques and they need slightly more computing time [2, 3].

This paper presents a new integration technique for gradient fields, which derives a depth map of an object for the multiple view directions in polar coordinates. Surface recovery from a sequence of images [11, 12] taken from different view directions is easy to implement and could provide accurate and reliable results. Section 2 describes the experimental setup and the principle of the new integration approach. Section 3 shows some experimental results. A conclusion is given in section 4.

2 Integration Technique in Polar Coordinates

This section is firstly to describe the experimental setup and conditions for our work. Then, the principle of the new approach is presented in detail. Moreover, the error handling of the algorithm is provided finally.

2.1 Experimental Setup

The imaging geometry of the new technique is shown in Fig. 1. The regarded object is put on a turntable whose rotation angle can be exactly controlled. The Y axis coincides with the rotation axis of the turntable. The camera viewing direction (the optical axis) is aligned with the Z axis. The illumination directions [4] are denoted by $\mathbf{s}_1$, $\mathbf{s}_2$, $\mathbf{s}_3 \in \Re^3$ and point towards the light sources. The three light sources are distant light sources with unified known radiances over time and illuminated area. A surface normal $\mathbf{n}$ is *illuminated* by a light source with illumination direction $\mathbf{s}$ if $\angle(\mathbf{s}, \mathbf{n}) \leq 90°$ holds, otherwise the surface normal is *not illuminated*. Since the camera is far away from the object in the scene, orthographic projection is applied. The images are taken when the object rotates on the turntable. The actions of taking images and rotating the object are synchronised by a computer program.

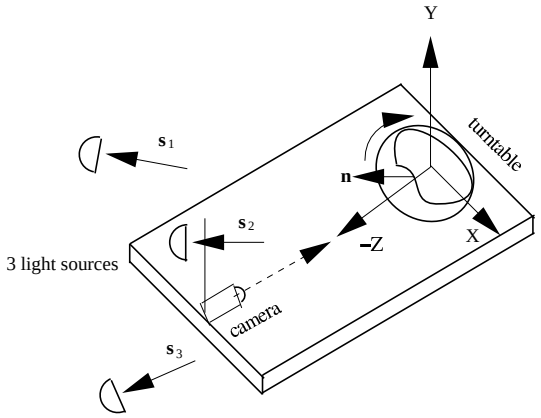

Figure 1: Experimental setup.

2.2 Principle of the Integration Technique

The new integration technique is to calculate the depth values of object surface points relative to the rotation axis with respect to the corresponding surface gradient in polar coordinates. The object on the turntable is rotated every $2\pi/n$ degree. The image is captured for every rotation. Each image can is digitised as $M \times N$ image grid. The surface normals of N row elements along the column coinciding with the rotation axis are calculated by photometric stereo method [1] in each of n images. Then, n sets of N gradient values compose a discrete $N \times n$ gradient field. This gradient field is used as input data for the new technique.

The new approach is related to a 3D model reconstruction method, the 360° profilometer, which results in the depth profiles of the considered surface points. At first, the depth values of the cross section of the object are integrated in 2D polar coordinates, i.e. the depth map is recovered slice by slice. Figure 2 (left) shows one cross section of the object in polar coordinates. The rotation axis is across the centre of the polar coordinates. One surface normal $\mathbf{n}$ of a pixel in the image plane is relative to one rotation angle $\beta =$ image number (i) $\times\, 2\pi/n$. So, the surface normal is denoted as function angle α with respect to the rotation angle β, i.e. $\alpha(\beta)$. α is the angle between surface slope and the view direction (or $-Z$). The region function d with respect to the rotation angle β and the gradient slope α, i.e. $d_\alpha(\beta)$, can be integrated from the known $\alpha(\beta)$.

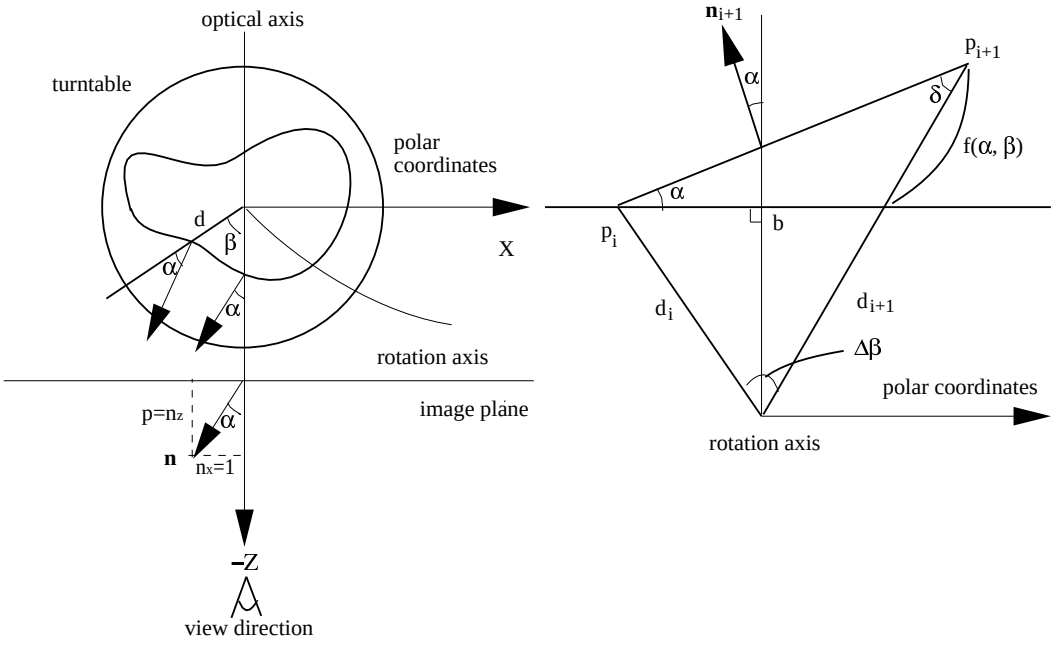

Figure 2: The basic geometry of depth map recovery of slice (left). Trigonometry relationship between two point p_i and p_{i+1} (right).

Calculation of $\alpha(\beta)$ depends on the $p = \frac{\partial Z}{\partial X}$ component of the surface gradient $(p,q)^T$, equivalently depends on the surface normal $\mathbf{n}$= $(n_X, n_Y, n_Z)^T$. This defines that one step in X coordinate means p steps in Z coordinate (see Fig. 2 (left)). Therefore, from trigonometry, $\alpha = \arctan\frac{1}{n_z} = \arctan\frac{1}{p}$. So, n gradient values of one row of the discrete $N \times n$ gradient field are applied to calculate $\alpha(\beta)$ of one slice.

Integration of depth map $d_\alpha(\beta)$ from $\alpha(\beta)$ in 2D polar coordinates is based on trigonometry (see Fig. 2 (right)). Supposing two successive points on the cross section p_i, p_{i+1}, the angle between these two points is $\Delta\beta = \frac{2\pi}{n}$. The radius of point p_i is d_i, while the radius of point p_{i+1} is d_{i+1}. The function $f(\alpha,\beta)$ denotes the difference between d_i and d_{i+1}. α_{i+1} is derived from the gradient value of point p_{i+1}. Given the depth value of the point p_i and calculated α_{i+1}, the depth value d_{i+1} of the point p_{i+1} is recovered by integrating along arbitrary curves in the plane

$$d_{i+1} = d_i + f(\alpha,\beta). \tag{1}$$

The function $f(\alpha,\beta)$ is derived by formula

$$\frac{b}{\sin\delta} = \frac{f(\alpha,\beta)}{\sin\alpha_{i+1}}, \tag{2}$$

where $\delta = \pi - \alpha_{i+1} - (\frac{\pi}{2} + \frac{\Delta\beta}{2}) = \frac{\pi}{2} - (\alpha_{i+1} + \frac{\Delta\beta}{2})$, $b = 2d_i\sin(\frac{\beta}{2})$. So, it holds

$$f(\alpha,\beta) = \frac{2d_i\sin(\frac{\Delta\beta}{2})}{\sin(\frac{\pi}{2} - \alpha_{i+1} - \frac{\Delta\beta}{2})} \cdot \sin(\alpha_{i+1}). \tag{3}$$

Therefore, the depth map calculation formula of new integration technique is

$$\begin{aligned} d_{i+1} &= d_i + d_i \cdot \frac{2d_i\sin(\frac{\Delta\beta}{2})}{sin(\frac{\pi}{2} - \alpha_{i+1} - \frac{\Delta\beta}{2})} \cdot \sin\alpha_{i+1} \\ &= d_i \cdot (1 + \frac{2d_i\sin(\frac{\Delta\beta}{2})}{\sin(\frac{\pi}{2} - \alpha_{i+1} - \frac{\Delta\beta}{2})} \cdot \sin\alpha_{i+1}). \end{aligned} \tag{4}$$

Hence, given initial depth value of the first point in the cross section whose angle in polar coordinates is zero and given the gradient values of considered points on the cross section, then the angle $\alpha(\beta)$ can be calculated from the surface gradient field, furthermore, the depth values of the corresponding points can be recovered by

$$d_{i+1} = d_i \cdot g(\alpha, \beta), \tag{5}$$

where $g(\alpha, \beta) = 1 + \frac{2d_i \sin(\frac{\Delta\beta}{2})}{\sin(\frac{\pi}{2} - \alpha_{i+1} - \frac{\Delta\beta}{2})} \cdot \sin\alpha_{i+1}$. Finally, combining the depth values of all slices together, the 360° depth profiles of the considered surface points form the discrete $N \times n$ depth map of the object.

2.3 Spreading Error

In one cross section, the point p_{n+1} is the same point as p_1, theoretically $d_{n+1} = d_1$, i.e. $d_1 \cdot g(\mathbf{n}_2) \cdot g(\mathbf{n}_3) \cdot g(\mathbf{n}_4) \ldots g(\mathbf{n}_{n+1}) = d_1$, then $\prod_{i=2}^{n+1} g(\mathbf{n}_i) = 1$. However, the measurement of the integration by equation (5) accumulates and distributes the errors along the calculation, practically $\prod_{i=2}^{n+1} g(\mathbf{n}_i) = \Delta$. The scheme of uniformly spreading the error is employed to reduce the accumulating error in depth values calculation.

$$\frac{g(\mathbf{n}_2)}{\sqrt[n]{\Delta}} \cdot \frac{g(\mathbf{n}_3)}{\sqrt[n]{\Delta}} \cdots \frac{g(\mathbf{n}_{n+1})}{\sqrt[n]{\Delta}} = 1. \tag{6}$$

So, given the first depth value d_1, the depth values for n points which are evenly distributed on the cross section are integrated as following

$$\begin{aligned} d_2 &= \frac{d_1 \cdot g(\mathbf{n}_2)}{\sqrt[n]{\Delta}} \\ d_3 &= \frac{d_1 \cdot g(\mathbf{n}_2) \cdot g(\mathbf{n}_3)}{(\sqrt[n]{\Delta})^2} \\ &\cdots \\ d_{n+1} &= \frac{d_1 \cdot g(\mathbf{n}_2) \cdot g(\mathbf{n}_3) \ldots g(\mathbf{n}_{n+1})}{(\sqrt[n]{\Delta})^n}. \end{aligned} \tag{7}$$

This is the error spreading scheme applied to refine the obtained depth values in the new method.

3 Experiments

The new integration algorithm is tested on reconstructing the single slice of the different mathematics models, such as polygon based model, continuous function based model, and the real object model Beethoven. The input data - gradient fields of the integration algorithm are generated by analytic differentiation for mathematics models or by photometric stereo method for the real object model.

3.1 Polygon Based Model

A polygon defined as formula $d(\beta) = 5 + \sin(4\beta)$ is introduced to recovering process. β is the angle of the considered point on this polygon and $d(\beta)$ is the true distance of this point in polar coordinates. The first point on the polygon starts at angle $\frac{\Delta\beta}{2}$, the following points dispersed on the polygon are separated evenly by angle $\Delta\beta = \frac{2\pi}{n}$. The normal $\mathbf{n}_{i+1}$ in Fig. 2 (right) is obtained by calculating the slopes of the lines between the two successive points.

3.2 Continuous Function Based Model

Continuous function $d(\beta) = 5 + \sin(4\beta)$ model is also used as input data. The normal values of the selected points of this function are obtained by continuous function normal calculation. For continuous

function $d(\beta)$ in polar coordinates, its corresponding x, z coordinates in cartesian coordinates are $x(\beta) = d(\beta) \cdot \cos(\beta)$, $z(\beta) = d(\beta) \cdot \cos(\beta)$, then, the differentiations of x and z with respect to β are $\dot{x}(\beta) = \dot{d}(\beta) \cdot \cos(\beta) + d(\beta)(-\sin(\beta))$, $\dot{z}(\beta) = \dot{d}(\beta) \cdot \sin(\beta) + d(\beta)\cos(\beta)$, respectively. Therefore, the normal $\mathbf{n}_{i+1}$ in Fig. 2 (right) is approximated by the normal of point p_{i+1}. It is calculated by $\mathbf{n}_{i+1} = (-\dot{z}_{i+1}, \dot{x}_{i+1})$. Let $n = 81$, Fig. 3 (left) shows the reconstructed result.

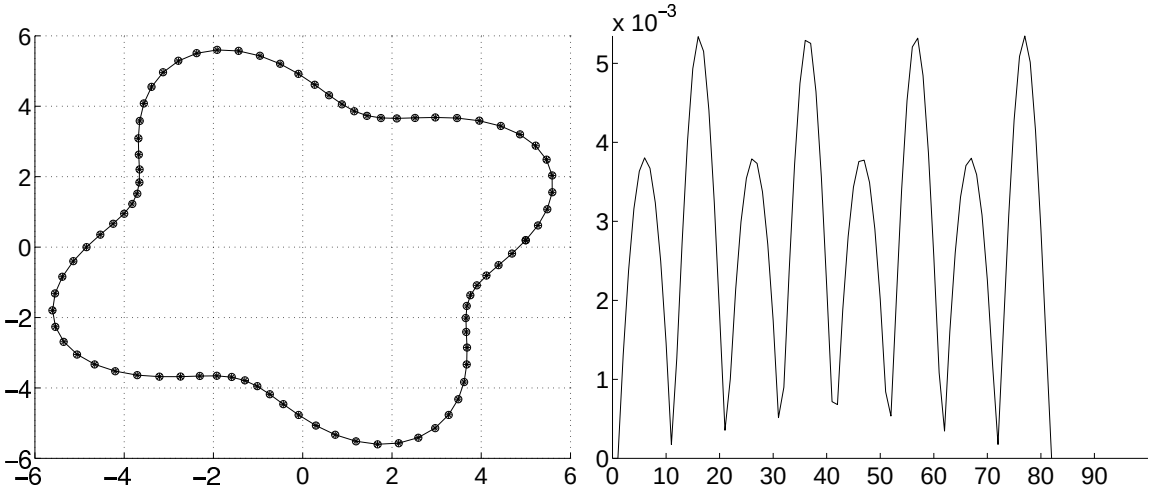

Figure 3: The reconstructed and the true distances of the regarded points of this continuous function in polar coordinates. $\circ$ represents the reconstructed points and $*$ represents the original points (left). The absolute differences between the reconstructed and the true distances of the selected points of the continuous function. x axis presents the number of the points. y axis presents the absolute difference of each point (right).

3.3 Real Object Model

In the next example, the new method is applied to the real object - Beethoven statue. In our experiments, we had $n = 81$, and $M = N = 256$. So, 81 images (256×256) are captured from the Beethoven bust which is on turntable and illuminated from three different light directions. The surface normals of 256 rows along the column coincided with the rotation axis in each image are calculated by photometric stereo algorithm. A discrete 256×81 gradient field given in polar coordinates is therefore obtained. To integrate depth values for one cross section, for example slice no. 122, only 81 surface normals of row 122 of this discrete 256×81 gradient field is input to the integration algorithm. The reconstruction of the cross section no. 122 is shown in Fig. 4.

4 Conclusion

The new integration method is invented to integrate depth map from the gradient field for the multiple view direction in polar coordinates. More generally speaking, the reconstructed depth map depends upon the accuracy of the gradient field and sounds reasonable for studied models. Errors in the generated gradient field may result in reconstruction errors for the new integration techniques. This points out that further improvements of shading based gradient calculations are required to ensure applications in 3D object modelling.

Acknowledgement: We sincerely thank Professor *Reinhard Klette* who provided essential advice, guidance and encouragement.

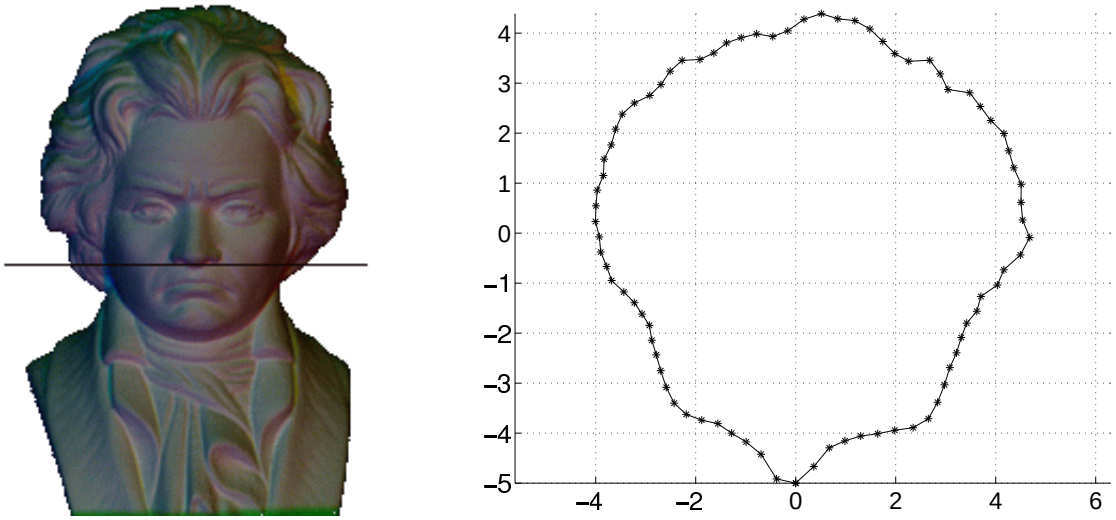

Figure 4: Object BEETHOVEN (left) and the reconstruction of one cross section of this object at the level of his nose tip (right).

References

[1] B. Horn, *Robot Vision*, The MIT Press, Cambridge, Massachusetts, 1992.

[2] R. Klette, K. Schlüns, *Height data from gradient fields*, SPIE Vol. 2908, "Machine Vision Applications, Architectures, and Systems Integration V", 18-19 November 1996, Boston, Massachusetts, pp.204-215.

[3] R. Klette, K. Schlüns, A. Koschau, *Computer Vision*, Springer, Singapore, 1998.

[4] K. Schlüns, *Shading based 3D shape recovery in the presence of shadows*, "Digital Image and Vision Computing: Techniques and Applications", 10-12 December 1997, Albany, Auckland, New Zealand (Massey University), pp.195-200.

[5] N. E. Coleman, Jr. and R. Jain *Obtaining 3-dimensional Shape of Textured and Specular Surfaces Using Four-Source Photometry*, CGIP, vol. 18, 1982, pp.309-328.

[6] R. T. Frankot and R. Chellappa *A Method for Enforcing Integrability in Shape from Shading Algorithms*, IEEE Transaction on Pattern Analysis and Machine Intelligence, vol. 10, 1988 pp.439-451.

[7] G. Healey and R. Jain *Depth Recovery from Surface Normals*, ICPR'84, Montreal, Canada, July 30-August 2, 1984, pp.894-896.

[8] B. K. P. Horn and M. J. Brooks *The Variational Approach to Shape from Shading*, CVGIP, vol. 33, 1986 pp.174-208.

[9] V. Rodehorst *Vertiefende Analyse eines Gestalts-Constraints von Aloimonos und Shulman*, Technischer Bericht, CV-Bericht 8, Institut für Technische Informatik, TU Berlin, 1993.

[10] Z. Wu, L. Li, *A Line-Integration Based Method for Depth Recovery from Surface Normal*, CVGIP, vol 43, 1988, pp.53-66.

[11] J. Lu, J. Little, *Reflectance Function Estimation and Shape Recovery from Image Sequence of a Rotating Object*, ICCV, Cambridge, MA, 20-23 June, 1995.

[12] J. Lu, J. Little, *Geometric and Photometric Constraints for Surface Recovery*, ICCV, San Francisci, USA, June, 1996.